

# Deep-Learning Estimation of Weight Distribution Using Joint Kinematics for Lower-Limb Exoskeleton Control

Clément Lhoste, Emek Barış Küçükatabak, Lorenzo Vianello, Lorenzo Amato, Matthew R. Short, Kevin M. Lynch, and Jose L. Pons

**Abstract**—In the control of lower-limb exoskeletons with feet, the phase in the gait cycle can be identified by monitoring the weight distribution at the feet. This phase information can be used in the exoskeleton’s controller to compensate the dynamics of the exoskeleton and to assign impedance parameters. Typically the weight distribution is calculated using data from sensors such as treadmill force plates or insole force sensors. However, these solutions increase both the setup complexity and cost. For this reason, we propose a deep-learning approach that uses a short time window of joint kinematics to predict the weight distribution of an exoskeleton in real time. The model was trained on treadmill walking data from six users wearing a four-degree-of-freedom exoskeleton and tested in real time on three different users wearing the same device. This test set includes two users not present in the training set to demonstrate the model’s ability to generalize across individuals. Results show that the proposed method is able to fit the actual weight distribution with  $R^2 = 0.9$  and is suitable for real-time control with prediction times less than 1 ms. Experiments in closed-loop exoskeleton control show that deep-learning-based weight distribution estimation can be used to replace force sensors in overground and treadmill walking.

**Index Terms**—Deep Learning, real-time control, lower-limb exoskeleton, rehabilitation robots, assistive robots

## I. INTRODUCTION

Lower-limb exoskeletons are increasingly being utilized in everyday tasks and rehabilitation for individuals with gait impairments. In clinical settings, these exoskeletons are typically classified into two main types: partial assistance and full mobilization. Full mobilization exoskeletons are designed for patients with severe motor control disorders, providing autonomous movement of the legs regardless of the patient’s input [1]. Conversely, partial assistance exoskeletons aid in

C. Lhoste and L. Vianello are with the Legs and Walking Lab, Shirley Ryan AbilityLab, Chicago, IL, USA.

E. B. Küçükatabak is with the Center for Robotics and Biosystems, Department of Mechanical Engineering, Northwestern University, Evanston, IL, USA and Shirley Ryan AbilityLab.

L. Amato is with the Shirley Ryan AbilityLab and the Biorobotics Institute, Scuola Superiore Sant’Anna, 56025 Pontedera, Italy and Department of Excellence in Robotics & AI, Scuola Superiore Sant’Anna, 56127 Pisa, Italy.

M. R. Short is with the Shirley Ryan AbilityLab and Department of Biomedical Engineering, Northwestern University, Evanston, IL, USA

K. M. Lynch is with the Center for Robotics and Biosystems and Department of Mechanical Engineering, Northwestern University.

J. L. Pons is with the Shirley Ryan AbilityLab, Center for Robotics and Biosystems, Department of Mechanical Engineering, Department of Biomedical Engineering, and Department of Physical Medicine and Rehabilitation, Northwestern University.

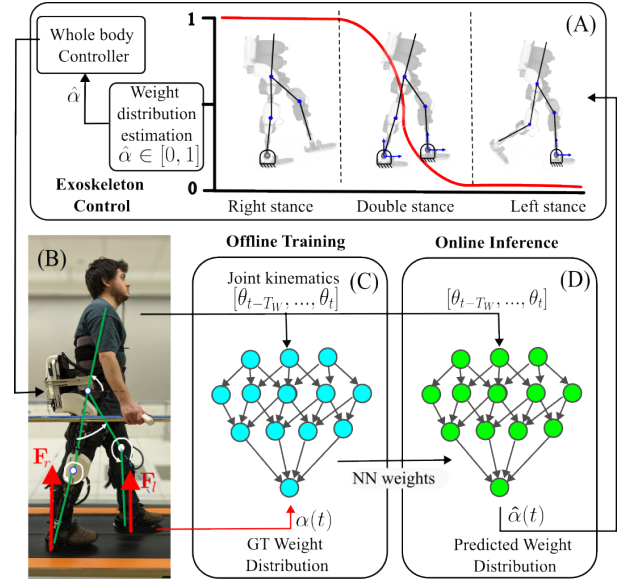


Fig. 1: Weight-distribution regression: a deep-learning approach is used to estimate the weight distribution ( $\alpha$ ) of a user-exoskeleton couple in real-time and to control the robot accordingly. Part (A) and (B) of the schema, Sec.II-A, provides an overview of the exoskeleton hardware and controller as well as the calculation of  $\alpha$  using force sensors applied to the feet and used as ground truth value. Part (C), Sec. II-B, presents the structure of the deep-learning model and its offline training using a time-window (300ms) of kinematics information as input and ground truth values of  $\alpha$  as output. Part (D), Sec II-C, displays how the trained model is used in the closed-loop control to predict the weight distribution ( $\hat{\alpha}$ ) using kinematic information. The estimated values are passed in real-time (inference time  $< 1$ ms) to the exoskeleton controller.

the patient’s movement while still requiring their active input. In this paper, we focus on partial assistance exoskeletons, as they are commonly employed in rehabilitation. Depending on the functional level of the patient, these exoskeletons use techniques like haptic guidance/assistance [2] or error augmentation/resistance [3] to facilitate the (re)learning of walking behaviors. Implementing both haptic assistance and resistance strategies requires precise control over the interaction torques between the user and the exoskeleton, ensuring effective and safe physical interaction.

Typically, the control of the interaction between a user and exoskeleton adopts a hierarchy of control levels: high-level, mid-level, and low-level [1], [4]. For lower-limb exoskeletons, the high-level controller calculates the desired interaction

torques tailored to specific ambulatory activities, such as walking on flat terrain, stairs or ramps. The role of the mid-level controller is to estimate the various states within an activity, for example, identifying the gait states (e.g., swing and stance) during walking and setting a desired interaction torque behavior accordingly. Finally, the low-level controller is responsible for compensating the exoskeleton’s dynamics and generating motor commands, based on the desired interaction torque profile identified by the mid-level controller.

In this three-level approach, an accurate, real-time estimation of the gait state in the mid-level and low-level is essential for properly controlling the exoskeleton. A common approach to gait state detection is to use gait events (e.g., heel strike, toe-off) to identify the switching between discrete gait states: left stance, right stance, and double stance [5], [6], [1]. However, achieving a smooth transition between these states is vital to ensure a control input that limits unexpected behaviors for the user. Küçüktabak et al. [7] proposed a whole-exoskeleton closed-loop compensation (WECC) controller that uses the ratio of ground reaction forces (GRF) (i.e., weight distribution) to approximate the double stance phase as a transition between the left and right stance. The weight distribution, quantified as the stance interpolation factor  $\alpha$ , smoothly changes from zero (left stance) to one (right stance) during double stance, as visualized in Fig. 1. Nonetheless, the requirement of additional sensors for GRF measurements, such as treadmill force plates or insoles, increases the complexity and cost of these systems.

Machine learning models have demonstrated their ability to estimate gait states using only joint kinematics of humans walking without exoskeletons, thus eliminating the need for GRF measurements [8], [9], [10]. Motivated by these results, recent studies have proposed real-time estimation of gait states with lower-limb exoskeletons. For instance, Jung et al. [11] and Liu et al. [12] used data from joint encoders and an inertial measurement unit (IMU) positioned on the trunk to classify the gait cycle during walking. These studies divided gait cycles into two (i.e., stance and swing) and eight gait states, respectively. However, discrete control states result in torque or modeling discontinuities. Camardella et al. [13] and Lippi et al. [14] address this issue by implementing a linear regression and a Neural Network model for regression with joint angles as inputs. The model’s output smoothly transitions between left and right stance, providing a continuous representation of the gait state. Despite this advancement, these approaches present some limitations. First, they only consider the present joint configuration, discarding past information. This approach might lead to inaccuracies in predictions as the weight distribution is influenced not only by the current posture, but also by the velocity and acceleration of the motion. Moreover, few considerations in these studies are given to the generalization across users and the prediction time performances. The latter is essential for real-time implementation of the exoskeleton’s whole-body controller.

To address the aforementioned limitations, we present a deep-learning approach for estimating the weight distribution of a user wearing a lower-limb exoskeleton. This approach utilizes a short time window of kinematic data extracted from sensors integrated in the exoskeleton. For the validation of

predictions, we compared the proposed approach with the method in [14] which only uses the instantaneous posture. Employing distinct users for training and testing resulted in a user-independent estimation, eliminating the need for a calibration phase. The proposed deep-learning method was trained on walking data from six users, and its closed-loop performance was evaluated on three users (two of which were not included in the training set) during treadmill and overground walking. The results showed that weight distribution can be accurately estimated using kinematic data with an  $R^2$  of 0.9 averaged across users. In addition, this approach was compatible with real-time requirements, achieving a prediction time less than 1 ms.

## II. METHODS

### A. Exoskeleton

We validated our proposed method on a commercially available lower-limb exoskeleton (ExoMotus-X2, Fourier Intelligence, Singapore). The exoskeleton system has four active degrees of freedom (DoF) at the hip and knee, and two passive DoFs at the ankle (Fig. 1B). The exoskeleton was modified to include strain gauges to estimate joint torques, and an Inertial Measurement Unit (IMU) on the backpack to measure the orientation of the trunk [7].

In this study, to measure GRFs, and therefore calculate weight distribution, two distinct devices were employed: a sensorized, split-belt treadmill and force-sensitive resistor (FSR) footplates. The treadmill is equipped with eight 3-DoF force plates (9047B, Kistler), offering highly accurate readings and a simple calibration process to zero the measured forces. However, its use restricts the practical applications of the exoskeleton and prevents its integration into overground scenarios. To address this limitation, FSR footplates were installed beneath the soles of the exoskeleton, facilitating the measurement of forces between the user-exoskeleton couple and the ground. Each footplate is equipped with 16 force-sensitive resistors, amounting to a total of 32 sensors across both footplates. These sensors interface with the ground through a rigid aluminum sole and rubber bearings, adding a degree of compliance. Although these sensors are more complex to calibrate and set up in comparison to the treadmill, they allow the exoskeleton to be used during overground walking.

GRFs enable the calculation of weight distribution in the user-exoskeleton couple. This allows an accurate and smooth transition between the left and right stance dynamic models of the exoskeleton (Fig. 1A). In this work, we calculated the weight distribution as the ratio of the vertical GRF of each foot similar to [7],

$$\alpha = \frac{F_{\text{right},y}}{F_{\text{left},y} + F_{\text{right},y}}, \quad (1)$$

where  $\alpha \in [0, 1]$  is the *stance interpolation factor*, while  $F_{\text{left},y}$  and  $F_{\text{right},y}$  represent the vertical GRFs.

Communication between motors and sensors is achieved using the CANOpen protocol. The controller is implemented on a ROS and C++ based open-source platform called the CANOpen Robot Controller (CORC) [15].

## B. Weight Distribution via Deep-Learning Regression

In an effort to simplify the equipment mounted on the exoskeleton, we propose a deep-learning approach to provide an estimate  $\hat{\alpha}$  of the stance interpolation factor using only kinematic information as input. Our approach is based on a Long Short-Term Memory (LSTM) network that uses a time window of kinematic values ( $x_t = [\theta_{t-T_W}, \dots, \theta_{t-t_1}, \theta_t]$ ) as input and returns the current  $y_t = \hat{\alpha}_t$  as an output. The vector ( $\theta$ ) is composed of the joint angles of the hip and knee joints for both legs, and the backpack angle in the sagittal plane ( $\theta = [\theta_{l\_hip}, \theta_{r\_hip}, \theta_{l\_knee}, \theta_{r\_knee}, \theta_b]$ ). To evaluate the effects of short-term history, models with a time window of  $T_W = 300$  ms (considering the recommendations from [16]) were compared with models  $T_W = 0$  ms that only use the instantaneous kinematic posture at time  $t$  (similar to [14]).

The architecture of the LSTM model is similar to the architecture in [17] and is presented in Fig. 2. The sensor data was sampled with a frequency of 333 Hz resulting in an input matrix of size (99,5) (99 time instances of five kinematic parameters) for the short-term history model and an output data of size (1,1). Gaussian noise (standard deviation of 0.01) is used in the first layer to introduce variability to the input data ( $x_t$ ), allowing better generalization. The LSTM layer allows the model to learn dependencies between the different time steps in the window of data. This layer is configured with 20 units. Finally, dense layers transform the features extracted from the LSTM to a single value representing the weight distribution ( $\hat{\alpha}_t$ ). A sigmoid activation function is used in these layers to always return a value between 0 and 1 in accordance with the definition of the *stance interpolation factor*; this provides a usable output from the network as an input to the control framework. Hyperparameters were selected using a heuristic approach. We employed leave-one-out cross-validation and used the coefficient of determination ( $R^2$ ) and Mean Square Error (MSE) between the predicted ( $\hat{\alpha}$ ) and actual ( $\alpha$ ) stance interpolation values as performance metrics to evaluate the chosen parameters.

The model was trained using the ADAM optimizer [18]. We utilized the MSE loss function to measure and minimize the discrepancy between the predicted ( $\hat{\alpha}$ ) and actual ( $\alpha$ ) values obtained from treadmill measurements. The training process was conducted over 10 epochs, processing the data in batches of 256 samples, to allow efficient weight adjustments while ensuring comprehensive coverage of the data. The LSTM model was trained using the TensorFlow library (v2.15.0, Google); we employed TensorFlow Lite (v2.13.0, Google) to make predictions in real time. The converted lite model is called by a Python script that runs in parallel to CORC in C++. The communication between these two components is achieved via ROS.

## C. Experimentation

We used data collected in two of our previous studies [7], [19] to select the parameters of the LSTM model trained offline (Fig. 1C) and then to validate its usability in real-time applications (Fig. 1D). The training data includes six users wearing the exoskeleton and walking for a total of

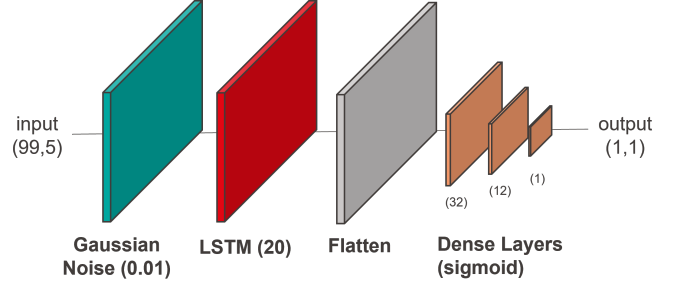


Fig. 2: Model architecture to predict the stance interpolation factor (parameters are shown in parentheses). Gaussian noise is used to corrupt the data and improve generalization. The LSTM layer extracts features in the temporal domain of the input. Dense layers serve as regression layers, transforming the features into the desired output. The input vector contains the last 300 ms kinematic information ( $[\theta_{t-T_W}, \dots, \theta_t]$ ) collected with a frequency of 333 Hz, resulting in an input vector of size (99,5). The output of the network is the stance interpolation factor ( $\alpha_t$ ) of size (1,1) at time  $t$ .

210 minutes. Users walked on a treadmill with a speed of 0.3 m/s either in the haptic transparent mode (i.e., zero desired interaction torques) or in a haptic rendering mode where virtual rotational spring-damper elements were rendered at their hip and knee joints [7]. The rendered virtual impedance has stiffness and damping values of 30 Nm and 6 Nms, and neutral position of  $25^\circ$  and  $-45^\circ$  at hip and knee, respectively. After the offline training and validation of prediction capability, we evaluated the capability of the LSTM network for closed-loop predictions of the stance interpolation factor  $\hat{\alpha}$  in two experiments.

In the first experiment, three users wore the exoskeleton and walked for one minute on a sensorized treadmill for each mode (i.e., haptic transparency and rendering). The stance interpolation factor for the exoskeleton controller was calculated either using the treadmill force plates as ground truth ( $\alpha$ ), or estimated using the LSTM model ( $\hat{\alpha}$ ). The measured or estimated value was used as an input to the WECC controller for interaction torque estimation and closed-loop compensation control in real-time [7]. The performance of the proposed model was assessed by comparing the spatiotemporal gait features and resultant interaction torque errors. Reported and visualized interaction torque errors in the plots are calculated using the ground truth  $\alpha$  obtained from the treadmill force plates, and divided by each user's weight. We report all performance values as the mean  $\pm$  standard deviation across users and steps unless otherwise specified. To assess the network's ability to generalize to unobserved walking conditions and different controllers, we evaluated the model on three speeds (0.14 m/s, 0.25 m/s, and 0.47 m/s) and two exoskeleton control modes (haptic transparency and rendering). Moreover, two of the three test users were not in the training set. Inter-user variability is removed from the presented box plots by demeaning the data of each condition/user pair and subsequently adding the overall mean of each condition, including three users.

In the second experiment, two users who were not featured in the training set performed trials of overground walking. The deep-learning approach was trained on a dataset of healthy

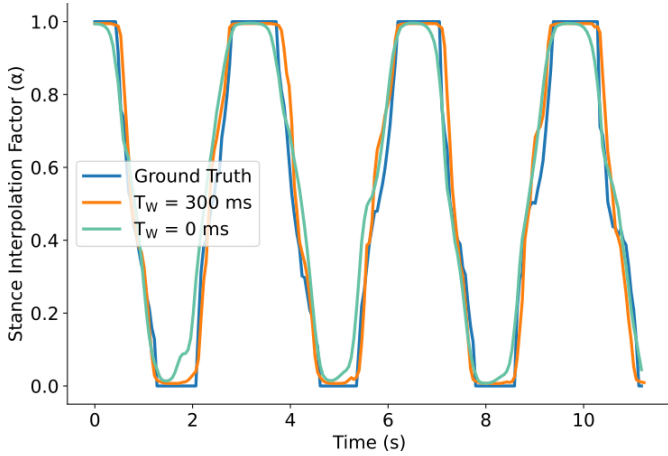


Fig. 3: Validation of stance interpolation factor predictions for a representative user (US<sub>4</sub>), using a window of 300 ms (orange) and with only the instantaneous joint configuration (green). Force plate condition (ground truth) is shown in blue.

individuals walking on a treadmill, thus we aim to demonstrate the model’s ability to generalize to more naturalistic walking behaviors. In this experiment,  $\alpha$  was calculated using the FSR footplates, while  $\hat{\alpha}$  was calculated using the deep-learning approach. The users walked for 10 meters at a self-selected speed, repeated three times for each condition; interaction torques and resultant joint angles were used to assess the performance.

### III. RESULTS

#### A. Validation of Deep-Learning Predictions

The proposed LSTM model was evaluated using a leave-one-out cross-validation approach: in each iteration, the model was trained on five users and then tested on the remaining user. In this test, we compared a model using instantaneous kinematic data ( $T_W = 0$  ms) and another using a history of kinematic data ( $T_W = 300$  ms). Fig. 3 shows the prediction for each model evaluated on the test set composed by User Four and the ground truth value.

The model using instantaneous kinematic data resulted in a prediction time of  $201 \pm 70.7$   $\mu$ s on a laptop (ThinkPad X1 Carbon 5th, Lenovo), while utilizing the history of kinematic data resulted in a prediction time of  $573 \pm 308$   $\mu$ s.

In terms of the prediction accuracy, the model incorporating a history of kinematic data produced a higher accuracy ( $T_W = 0$  ms:  $R^2 = 0.84 \pm 0.03$ ,  $MSE = 1.8 \times 10^{-2} \pm 0.4$ ;  $T_W = 300$  ms:  $R^2 = 0.90 \pm 0.02$ ,  $MSE = 1.1 \times 10^{-2} \pm 0.3$ ). Tab. I provides a detailed report of the model’s accuracy for individual users. Specifically, it includes MSE performances for both the training and test sets for  $T_W = 0$  ms and  $T_W = 300$  ms conditions.

#### B. Closed-Loop Performance During Treadmill Walking

After validation of the deep-learning predictions, we compared the closed-loop performance of the proposed method for  $\hat{\alpha}$  estimation and the measured ground truth  $\alpha$  from the treadmill force plates. Specifically, estimated or measured stance

Train-Set	Test-Set	$T_W = 0$ ms		$T_W = 300$ ms	
		Train	Test	Train	Test
US <sub>2,3,4,5,6</sub>	US <sub>1</sub>	0.0154	0.0199	0.0068	0.0146
US <sub>1,3,4,5,6</sub>	US <sub>2</sub>	0.0156	0.0182	0.0072	0.0109
US <sub>1,2,4,5,6</sub>	US <sub>3</sub>	0.0163	0.0133	0.0075	0.0082
US <sub>1,2,3,5,6</sub>	US <sub>4</sub>	0.0160	0.0176	0.0072	0.0125
US <sub>1,2,3,4,6</sub>	US <sub>5</sub>	0.0150	0.0234	0.0067	0.0123
US <sub>1,2,3,4,5</sub>	US <sub>6</sub>	0.0180	0.0126	0.0068	0.0081

TABLE I: Prediction accuracy expressed as MSE for the LSTM model (for training and testing set) with time window of 300 ms and instantaneous values. We performed a cross-user generalization evaluation by iteratively training on all users (US<sub>*i*</sub>) except one and testing on the excluded user.

interpolation factor values were used as inputs to the WECC controller [7] and resulting kinematics and interaction torque errors were evaluated during walking. During the closed-loop tests, we focused on the model with  $T_W = 300$  ms due to its improved accuracy compared to  $T_W = 0$  ms, while still obtaining a prediction time suitable for real-time implementation (0.57 ms).

In Fig. 4, we illustrate the stance interpolation factor with respect to normalized gait duration under different conditions. The stance interpolation factor values obtained from treadmill force plates and the deep-learning approach are displayed for three different speeds (0.14 m/s, 0.25 m/s, 0.47 m/s). Compared to using force plate values, the proposed method resulted in longer stance time during slower walking and shorter stance time during faster walking. At 0.14 m/s, stance duration was  $56.0 \pm 4.8\%$  of the gait cycle using the treadmill force plates versus  $67.1 \pm 9.7\%$  using deep learning. At 0.25 m/s, stance duration was similar between the two approaches:  $59.6 \pm 6.99\%$  of the gait cycle using the treadmill force plates, and  $65.1 \pm 1.6\%$  using deep learning. Finally, at 0.47 m/s, the treadmill force plates resulted in a stance duration of  $69.3 \pm 10.2\%$  versus  $59.7 \pm 5.74\%$  using deep learning.

Interaction torque errors were investigated to evaluate the quality of the haptic rendering and transparency, using the force plates and the deep-learning predictions for the stance interpolation factor in real time. Fig. 5 presents the interaction torque tracking performance during the rendering mode while using the force plate measurements and deep-learning estimation in the dynamic robot model. It was observed that interaction torque error is higher with the deep-learning method at the start of the swing. Specifically, toe-off (60-70% of the gait cycle) led to an average hip interaction torque error of 0.068 Nm/kg using force plates and 0.109 Nm/kg using deep learning. However, this error was lower for the deep-learning approach in the stance phase. Within the 20-50% range of the gait cycle, the average hip interaction error was 0.111 Nm/kg using force plates and 0.033 Nm/kg using deep learning. The mean of the interaction torque error over the whole cycle, across three users, was comparable between the two conditions. At the hip joint, mean absolute interaction torque errors of  $0.101 \pm 0.004$  Nm/kg and  $0.094 \pm 0.005$  Nm/kg were observed with the deep-learning and force plate conditions, respectively. Similarly, the mean absolute interaction torque error at the knee joint was  $0.119 \pm 0.006$  Nm/kg and  $0.113 \pm 0.006$  Nm/kg for the deep-learning and force plate conditions.

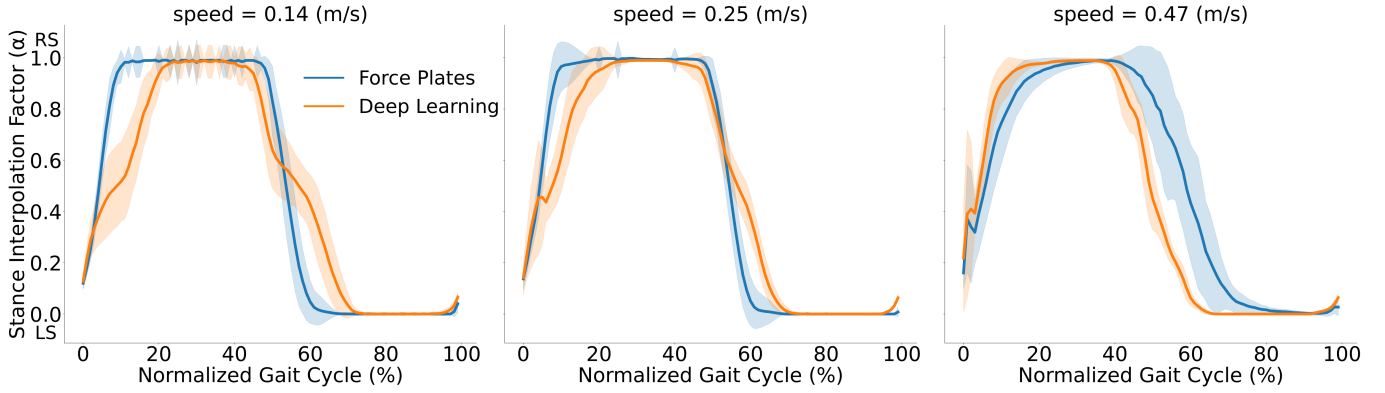


Fig. 4: Stance interpolation factor using the treadmill force plates (blue) and using the deep-learning prediction (orange) for closed-loop exoskeleton control. Shaded error bars indicate  $\pm$  one standard deviation relative to the mean. RS and LS denote Right Stance ( $\alpha = 1$ ) and Left Stance ( $\alpha = 0$ ), respectively. User walked at 0.14 m/s, 0.25 m/s and 0.47 m/s for one minute in every condition.

Fig. 6 shows the results of the transparency performances on both conditions. The deep-learning approach resulted in a relatively smaller hip interaction torque error compared to the force-plate condition ( $0.063 \pm 0.006$  Nm/kg vs.  $0.073 \pm 0.008$  Nm/kg). On the other hand, the deep-learning approach resulted in a higher interaction torque error at the knee joints between 60% and 70% of the normalized gait, corresponding to the beginning of the swing phase. The mean knee interaction torque error in this period was  $-0.207$  Nm/kg for the force plate condition and  $-0.312$  Nm/kg for the deep-learning approach. Users also qualitatively reported that the exoskeleton felt heavier at this particular moment of the gait cycle. Across the whole gait cycle, the mean interaction torque error for the knee joint was similar for the deep-learning and the force plate conditions ( $0.078 \pm 0.007$  Nm/kg vs.  $0.071 \pm 0.007$  Nm/kg).

### C. Closed-Loop Performance During Overground Walking

During the overground tests, it was observed that the users preferred to walk at a slightly faster speed using the FSR footplates ( $0.241 \pm 0.024$  m/s) compared to the deep-learning estimation ( $0.198 \pm 0.020$  m/s). Results from Fig. 7B show similar kinematic patterns between the two conditions, particularly in the magnitudes of the joint angles. In the temporal domain, a longer stance period was observed with the deep-learning approach ( $75.3 \pm 2.7\%$ ) compared to the FSR condition ( $63.1 \pm 1.6\%$ ). Furthermore, Fig. 7 presents the interaction torque error over a gait cycle, for a representative user, using FSRs or deep learning. The interaction torque error, averaged over two users, was higher for the deep-learning condition (Hip:  $0.094 \pm 0.009$  Nm/kg using FSR and  $0.120 \pm 0.014$  Nm/kg using deep learning; Knee:  $0.083 \pm 0.007$  Nm/kg using FSR and  $0.116 \pm 0.009$  Nm/kg using deep learning).

## IV. DISCUSSION

In this paper, we evaluated a deep-learning model to predict the weight distribution (i.e., stance interpolation factor) of a user wearing a lower-limb exoskeleton during several walking conditions; we compared the exoskeleton controller performance when this stance interpolation factor was estimated with our deep-learning model ( $\hat{\alpha}$ ) and measured with ground truth

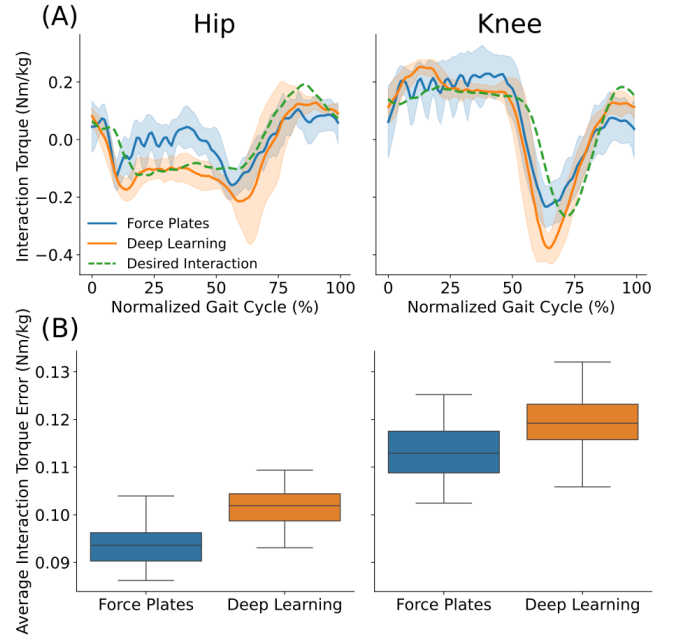


Fig. 5: Haptic rendering performance of the proposed deep-learning method during treadmill walking. (A) Interaction torque across normalized gait cycle for a representative user, walking at 0.25 m/s. The interaction torque highlights haptic rendering performances using treadmill force plates (blue) or deep-learning estimation (orange). Shaded error bars indicate  $\pm$  one standard deviation relative to the mean. Desired Interaction (in green) contains data from both treadmill force plates and deep-learning conditions. (B) Mean interaction torque error per step, for three users walking at 0.25 m/s. The boxplot shows highlights the interaction torque error in treadmill force plates and deep-learning conditions across users.

values (treadmill force plates or FSR sensor pads,  $\alpha$ ). This work highlights the viability and limitations of using deep-learning predictions to detect changes in the gait state using only joint kinematics information without ground reaction sensors.

Utilizing a history of kinematic data was shown to enhance

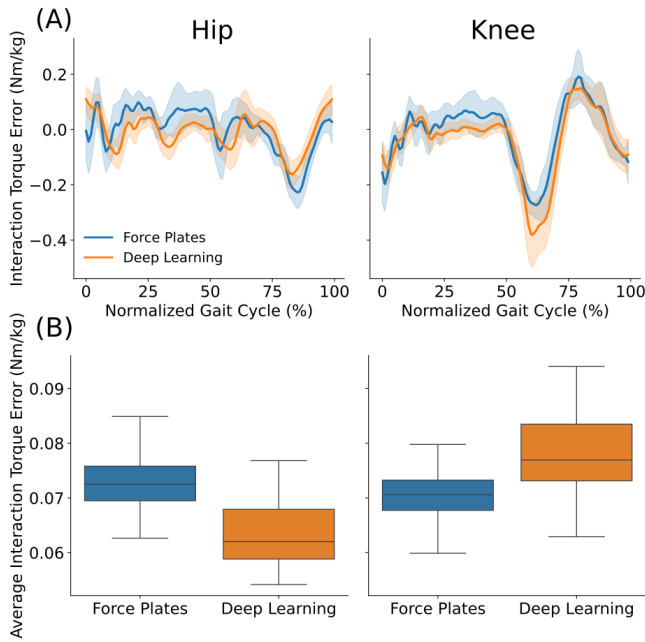


Fig. 6: Haptic transparency performance of the proposed deep-learning method during treadmill walking (desired interaction torque is zero). (A) Interaction torque error with respect to normalized gait cycle for a representative user walking at 0.25 m/s. Shaded error bars indicate  $\pm$  one standard deviation relative to the mean. (B) Boxplot of mean interaction torque error over each step, at 0.25 m/s. Results are aggregated over three users.

the model’s accuracy (Fig. 3 and Tab. I) in comparison to using instantaneous values, as seen in a similar study [14]. These findings show the advantage of utilizing additional temporal data from previous time steps, enhancing the network’s performance in both training and testing phases. Importantly, including additional data did not significantly alter the model’s prediction speed; we observed comparable prediction times when using a history of kinematic data with respect to the instantaneous value predictions.

As a result, the model was implemented to achieve real-time performance. This is crucial for its use in the control of an exoskeleton, as predictions need to be faster than the main control loop. Achieving an average prediction time of 0.57 ms ensured the real-time usability of the system, as the main control loop runs usually significantly slower than 1 ms on lower-limb exoskeletons (e.g., 3 ms for the exoskeleton controller in our study). It is noteworthy that, without using TensorFlow Lite (i.e., employing the classic TensorFlow library), the average prediction time with a history of kinematic data is  $67.1 \pm 13.5$  ms, which cannot be used in most real-time applications. Furthermore, the proposed method provides accurate predictions of the stance interpolation factor for previous and unseen users (Fig. 3 and Tab. I), demonstrating another aspect of its usability. Requiring training data for every exoskeleton user is not convenient or realistic, particularly in physical rehabilitation as a patient’s time spent receiving therapy must be prioritized.

In the context of machine learning for robotic control, using

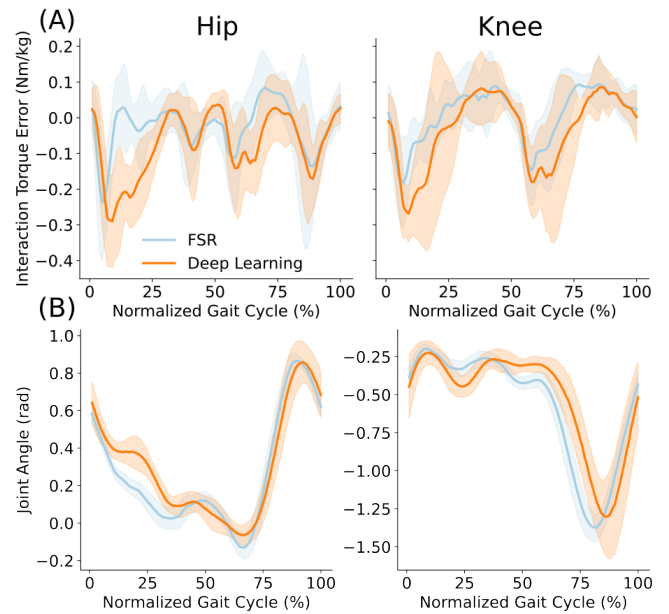


Fig. 7: Haptic transparency performance of the proposed deep-learning method during overground walking. (A) Interaction torque across normalized gait cycle, for a representative user, during overground walking. (B) Hip and Knee joint angles obtained with deep learning (orange) and FSR pad sensors (blue) conditions for a representative user. Shaded error bars indicate  $\pm$  one standard deviation relative to the mean.

the predictions in a closed loop can affect the performance due to error propagation in real time [20]. Therefore, it was critical to evaluate the closed-loop performance of our system, using several conditions. We demonstrated that the deep-learning approach produces a similar stance interpolation factor compared to treadmill force plates during walking with haptic transparent control; these findings generalize for walking speeds between 0.14 and 0.47 m/s (Fig. 4). To characterize the effect of the deep-learning predictions on the performance of the exoskeleton controller, we assessed both haptic rendering of nonzero impedance and haptic transparent modes during treadmill walking. Moreover, we evaluated the extent to which these results generalize to overground walking. During treadmill walking, mean interaction torque errors were similar between deep-learning predictions and treadmill force plate measurements. Evaluating the performance of the controller during more naturalistic, overground walking, the deep-learning predictions also facilitated similar interaction torque error profiles (Fig. 7A) and hip and knee kinematics (Fig. 7B).

While the overall performance of the exoskeleton controller was comparable when implementing our deep-learning predictions and ground reaction sensor values, we did observe a delay-like effect in the stance interpolation factor estimation which likely resulted in some performance discrepancies at specific phases of the gait cycle. Specifically, we observed a longer stance duration when walking with the deep-learning predictions at slower speeds (Fig. 4); this was associated with a longer transition between left and right single stance (i.e., double stance to swing).

During treadmill and overground walking, at the knee joint, we observed higher interaction torque error at the beginning of the swing phase (around 60-70% of the cycle, Fig. 6A) with the deep-learning predictions. This increase in interaction torque error was more noticeable during overground walking, and also observed at the hip joint. In this condition, the use of crutches may have promoted additional lateral movement which was not measured by the exoskeleton [21].

For both treadmill and overground walking, the discrepancies in interaction torque errors relative to their respective ground truths could be due to the deep-learning model requiring users to change their kinematics before the stance interpolation factor changes. This is different from using force sensors, which can detect changes in weight distribution independent of kinematics recorded by the exoskeleton. One way to improve the detection of changes in weight distribution in the deep-learning model is to incorporate the frontal plane IMU angle of the backpack in addition to the sagittal plane angles from the backpack and joint encoders.

## V. CONCLUSION

In this study, we demonstrated the feasibility of employing deep learning in gait state detection for exoskeleton control, eliminating the necessity of ground reaction force sensors. Despite challenges such as a limited dataset, real-time constraints, and issues related to error propagation, these obstacles were successfully addressed. Evaluation of our model's closed-loop performance versus typical sensors (i.e., force plates, FSR footplates) highlights the system's applicability across new users and several walking speeds and conditions. To address our model limitations, future work could include training datasets encompassing various walking speeds, overground walking and other activities (e.g. ramps, stairs). Furthermore, this work could be used to implement a state machine that utilizes an estimated stance interpolation factor, selecting impedance parameters in the mid-level controller for exoskeleton control and tailored assistance during walking. The proposed framework will be validated in future on additional healthy individuals as well as individuals with lower-limb impairments (e.g., stroke, spinal cord injury).

## ACKNOWLEDGMENT

This work was supported by the National Science Foundation / National Robotics Initiative (Grant No: 2024488). We would like to thank Tim Haswell for his technical support on the hardware improvements of the ExoMotus-X2 exoskeleton.

## REFERENCES

[1] R. Baud, A. R. Manzoori, A. Ijspeert, and M. Bouri, "Review of control strategies for lower-limb exoskeletons to assist gait," *Journal of NeuroEngineering and Rehabilitation*, vol. 18, no. 1, Jul. 2021. [Online]. Available: <https://doi.org/10.1186/s12984-021-00906-3>

[2] J. de Miguel-Fernández, J. Lobo-Prat, E. Prinsen, J. M. Font-Llagunes, and L. Marchal-Crespo, "Control strategies used in lower limb exoskeletons for gait rehabilitation after brain injury: a systematic review and analysis of clinical effectiveness," *Journal of NeuroEngineering and Rehabilitation*, vol. 20, no. 1, Feb. 2023.

[3] E. Basalp, P. Wolf, and L. Marchal-Crespo, "Haptic training: Which types facilitate (re)learning of which motor task and for whom? answers by a review," *IEEE Transactions on Haptics*, vol. 14, no. 4, pp. 722–739, 2021.

[4] M. Kim, A. M. Simon, and L. J. Hargrove, "Seamless and intuitive control of a powered prosthetic leg using deep neural network for transfemoral amputees," *Wearable Technologies*, vol. 3, 2022.

[5] W. Huo, S. Mohammed, Y. Amirat, and K. Kong, "Fast gait mode detection and assistive torque control of an exoskeletal robotic orthosis for walking assistance," *IEEE Transactions on Robotics*, vol. 34, no. 4, pp. 1035–1052, 2018.

[6] A. Ortlieb, R. Baud, T. Tracchia, B. Denking, Q. Herzig, H. Bleuler, and M. Bouri, "An active impedance controller to assist gait in people with neuromuscular diseases: Implementation to the hip joint of the autonomy exoskeleton," in *2018 7th IEEE International Conference on Biomedical Robotics and Biomechanics (Biorob)*, 2018.

[7] E. B. Küçüktabak, Y. Wen, S. J. Kim, M. R. Short, D. Ludvig, L. Hargrove, E. J. Perreault, K. M. Lynch, and J. L. Pons, "Haptic transparency and interaction force control for a lower-limb exoskeleton," *IEEE Transactions on Robotics*, pp. 1–19, 2024.

[8] M. Mundt, A. Koeppe, S. David, F. Bamer, W. Potthast, and B. Markert, "Prediction of ground reaction force and joint moments based on optical motion capture data during gait," *Medical Engineering & Physics*, vol. 86, pp. 29–34, 2020.

[9] A. Karatsidis, G. Bellusci, H. Schepers, M. de Zee, M. Andersen, and P. Veltink, "Estimation of ground reaction forces and moments during gait using only inertial motion capture," *Sensors*, vol. 17, no. 12, p. 75, Dec. 2016. [Online]. Available: <https://doi.org/10.3390/s17010075>

[10] L. Mouro, L. Hoyet, F. L. Clerc, and P. Hellier, "Underpressure: Deep learning for foot contact detection, ground reaction force estimation and footskate cleanup," *Computer Graphics Forum*, vol. 41, no. 8, pp. 195–206, 2022.

[11] J.-Y. Jung, W. Heo, H. Yang, and H. Park, "A neural network-based gait phase classification method using sensors equipped on lower limb exoskeleton robots," *Sensors*, vol. 15, no. 11, pp. 27738–27759, 2015.

[12] D.-X. Liu, X. Wu, W. Du, C. Wang, and T. Xu, "Gait phase recognition for lower-limb exoskeleton with only joint angular sensors," *Sensors*, vol. 16, no. 10, p. 1579, Sep. 2016.

[13] C. Camardella, F. Porcini, A. Filippeschi, S. Marcheschi, M. Solazzi, and A. Frisoli, "Gait phases blended control for enhancing transparency on lower-limb exoskeletons," *IEEE Robotics and Automation Letters*, vol. 6, no. 3, pp. 5453–5460, 2021.

[14] V. Lippi, C. Camardella, A. Filippeschi, and F. Porcini, "Identification of gait phases with neural networks for smooth transparent control of a lower limb exoskeleton," in *Proceedings of the 18th International Conference on Informatics in Control, Automation and Robotics - Volume 1: ICINCO*, INSTICC. SciTePress, 2021, pp. 171–178.

[15] J. Fong, E. B. Küçüktabak, V. Crocher, Y. Tan, K. M. Lynch, J. L. Pons, and D. Oetomo, "Canopen robot controller (corc): An open software stack for human robot interaction development," in *Wearable Robotics: Challenges and Trends*, J. C. Moreno, J. Masood, U. Schneider, C. Maufray, and J. L. Pons, Eds. Cham: Springer International Publishing, 2022, pp. 287–292.

[16] F. Labarrière, E. Thomas, L. Calistri, V. Optasanu, M. Gueugnon, P. Ornetti, and D. Laroche, "Machine learning approaches for activity recognition and/or activity prediction in locomotion assistive devices—a systematic review," *Sensors*, vol. 20, no. 21, 2020.

[17] M. Kim and L. J. Hargrove, "Deep-learning to map a benchmark dataset of non-amputee ambulation for controlling an open source bionic leg," *IEEE Robotics and Automation Letters*, vol. 7, no. 4, pp. 10597–10604, 2022.

[18] D. P. Kingma and J. Ba, "Adam: A method for stochastic optimization," *arXiv preprint arXiv:1412.6980*, 2014.

[19] E. B. Küçüktabak, Y. Wen, M. Short, E. Demirbaş, K. Lynch, and J. Pons, "Virtual physical coupling of two lower-limb exoskeletons," in *2023 International Conference on Rehabilitation Robotics (ICORR)*, 2023, pp. 1–6.

[20] S. Levine, A. Kumar, G. Tucker, and J. Fu, "Offline reinforcement learning: Tutorial, review, and perspectives on open problems," *arXiv preprint arXiv:2005.01643*, 2020.

[21] R. A. Alamro, A. E. Chisholm, A. M. M. Williams, M. G. Carpenter, and T. Lam, "Overground walking with a robotic exoskeleton elicits trunk muscle activity in people with high-thoracic motor-complete spinal cord injury," *Journal of NeuroEngineering and Rehabilitation*, vol. 15, no. 1, Nov. 2018.